

The crystal-structure and vacancy distribution in 6C pyrrhotite

JOHAN P.R. DE VILLIERS^{1,*} AND DAVID C. LILES²

¹Department of Materials Science and Metallurgical Engineering, University of Pretoria, Pretoria, 0002 South Africa

²Department of Chemistry, University of Pretoria, Pretoria, 0002 South Africa

ABSTRACT

The crystal structure of a 6C pyrrhotite from Mponeng Mine, South Africa, has been refined using starting atomic parameters postulated by Koto et al. (1975). This pyrrhotite is monoclinic and is described in the non-standard space group Fd , so that the metrically orthorhombic unit-cell shape is preserved. The cell symmetry is monoclinic with dimensions $a = 6.897(2)$, $b = 11.954(3)$, $c = 34.521(7)$, and with $\beta = 90.003(4)^\circ$. The structure has been refined with anisotropic displacement parameters to $R = 0.029$ using 1493 observable reflections with $I > 2\sigma(I)$ and $R = 0.034$ for all 1800 reflections. The internal R_{int} is 0.023 for the symmetrically equivalent reflection data. The composition of the crystal, as determined by electron microprobe analysis is $\text{Fe}_{10.91}\text{Ni}_{0.05}\text{S}_{12}$.

The crystal structure resembles that of the 5C pyrrhotite in that the atomic positions of the Fe and S atoms are arranged in a very similar fashion, the only real difference being the arrangement of partially occupied iron sites. The coordination of the iron atoms is octahedral and short Fe-Fe distances along the c -axis are also encountered in this structure.

The vacancy distribution is similar to that postulated by Koto et al. (1975) and is characterized by the stacking of two approximately half-occupied sites, followed by an essentially fully occupied layer. This is however a simplification and results in a composition that is too metal-rich. Two other slightly defect sites with occupancies of 0.90 and 0.87 are also present in the structure, and all layers contain both fully occupied and partially occupied sites. Refinement of the occupancies of all these sites gives rise to an atomic distribution that resembles the measured composition most closely, and is refined as $\text{Fe}_{10.99}\text{S}_{12}$.

The powder diffraction pattern of this structure is compared to the very similar pattern of the 5C structure. The crystal structure is also given in the more conventional Cc setting so as to be compatible with the available crystallographic software that cannot normally accommodate the Fd space group.

Keywords: Pyrrhotite-6C, crystal structure, non-stoichiometry, iron sulfide, superstructure

INTRODUCTION

Pyrrhotite is one of the most common sulfide minerals and is present as an accessory mineral in most rocks. It is a common mineral in most sulfide ore deposits, especially in those that contain Ni, Cu, and Pt group elements. To study the behavior of pyrrhotite in extraction processes, it is important to adequately characterize the members of this group of minerals.

Pyrrhotites, together with troilite, occur as minerals with various superstructures in nature. It is typically non-stoichiometric in composition with general formula Fe_{1-x}S , with x varying between 0 and 0.125. The minerals occur as the ordered 4C, 5C, and 6C varieties, where C represents the NiAs unit cell that is the subcell on which the structures of the group are based. These superstructures are not true polytypes because the occupancies of the layers differ in each superstructure, which is a consequence of the specific vacancy distribution.

The composition of the magnetic 4C structure, is ideally Fe_7S_8 with a Fe/S ratio of 0.875, but with a substantial compositional range from a Fe/S of 0.855 to 0.885, and is described in the non-standard $F2/d$ space group (Tokonami et al. 1972). It is also

described in the conventional $C2/c$ space group setting by Powell et al. (2004) in their neutron diffraction study of the magnetic properties of this pyrrhotite. The structure consists of alternating layers of filled Fe-S octahedra and layers containing one-third vacant Fe sites and two-thirds filled Fe-S octahedra. It must be mentioned that the above structure defines a stoichiometric composition (Fe_7S_8) and does not allow for a variable composition as is found in nature.

The structure of 5C pyrrhotite was determined by de Villiers et al. (2009), and this again shows a compositional range with Fe/S that spans across the ideal Fe_9S_{10} composition (Fe/S = 0.90) from 0.885 to 0.91. The structure contains two layers containing vacant Fe sites and all other layers consist of a mixture of sites with variable Fe occupancy together with fully occupied sites. The so-called “hexagonal pyrrhotite” is non-magnetic and is actually orthorhombic with space group $Cmce$ (formerly $Cmca$) as described originally by Morimoto et al. (1975), in their review of the pyrrhotites. The crystallography of the pyrrhotites is reviewed in more detail in the paper by de Villiers et al. (2009).

The structure of the 6C pyrrhotite was correctly postulated by Koto et al. (1975) as well as the broad details of the vacancy arrangement. Unfortunately, however, they did not give a full structure determination with unit cell, space group, and a list of

* E-mail: johan.devilliers@up.ac.za

refined atomic positions. They give the composition as $\text{Fe}_{11}\text{S}_{12}$ with a monoclinic, but metrically orthorhombic cell and the non-standard Fd space group. Again the compositions span a range across the ideal composition ($\text{Fe}/\text{S} = 0.917$) with Fe/S from 0.91 to 0.94.

The determination of the pyrrhotite structures forms part of a broader study of the electrochemical and flotation properties of pyrrhotite. Proper characterization and examination of pure samples of these superstructures are therefore essential for the understanding of their behavior. In addition, because of the similarity of the powder X-ray diffraction patterns of the non-magnetic (NC) pyrrhotites, which vary from Fe_9S_{10} to $\text{Fe}_{11}\text{S}_{12}$, their structural characterization is essential for the interpretation of the patterns and for their possible quantification. This study describes the structure of the 6C pyrrhotite and its vacancy distribution and compares it to that of the 4C and 5C superstructures.

EXPERIMENTAL METHODS

A sample of 6C pyrrhotite from the Mponeng gold mine was obtained from Bruce Cairncross of the University of Johannesburg, and this consisted of large ($1 \times 1 \times 0.1 \text{ cm}^3$) hexagonally shaped single crystals. A subsample was crushed and a small fragment was found to be suitable for single-crystal analysis. A fragment of the same single crystal was analyzed by a Cameca SX100 electron microprobe at the University of Pretoria, run at 20 kV accelerating voltage and 20 nA probe current. The average analysis for the crystal is 38.35 mass% for S, 60.71% for Fe, and 0.32% for Ni, which gives a composition $\text{Fe}_{10.91}\text{Ni}_{0.05}\text{S}_{12}$.

The unit cell was determined and diffraction data were collected using the Fd setting suggested by Koto et al. (1975) to retain the metrically orthorhombic setting. Data were collected on a Bruker (Siemens) P4 diffractometer equipped with a Bruker SMART 1K CCD detector using graphite-crystal monochromatized $\text{MoK}\alpha$ radiation by means of a combination of ϕ and ω scans. Data reduction was performed using SAINT+ (Bruker 2001), and the intensities were corrected for absorption by multiple scans of symmetry equivalent reflections using SADABS (Bruker 2001). The intensities of 3186 reflections were measured to obtain the 1800 unique reflections used in the refinements and the internal discrepancy factor of $R_{\text{int}} = 0.023$ was obtained, which was considered to be acceptable. Refinement was

done using SHELX97 (Sheldrick 1997), and the crystal data are given in Table 1. CIF¹ files are on deposit.

Refinement proceeded with the ideal starting positional parameters of the iron and sulfur atoms as suggested by Koto et al. (1975). Initially overall isotropic atomic displacement parameters for the iron and sulfur atoms, respectively, were used while refining positional parameters of all atoms and occupancies for the iron atoms. The occupancies of those iron atoms that refined close to unity were fixed as such and occupancies of four atomic sites were further refined. Individual isotropic displacement parameters were then introduced, and finally, anisotropic displacement parameters (ADPs). Final refinement consisted of a scale factor, a twin refinement with transformation matrix (1 0 0, 0 -1 0, 0 0 -1) and positional parameters and ADPs, together with occupancies of four Fe atoms, refined simultaneously. Final R -values of 0.029 using 1493 reflections with $I > 2\sigma(I)$ and $R = 0.034$ for all 1800 reflections were obtained. The goodness of fit value was $S = 1.084$ for the refinement of 222 parameters. The calculated composition obtained from the refinement was $\text{Fe}_{10.99}\text{S}_{12}$ with a standard deviation of 0.06 in the Fe composition as compared to the analyzed composition of $\text{Fe}_{10.91}\text{Ni}_{0.05}\text{S}_{12}$. The standard deviation in (Fe+Ni) is 0.11 for the analyzed crystal.

The model of Koto et al. (1975) with two iron atoms having half occupancies and all others fully occupied was also tested and gave $R = 0.035$ for 1493 reflections with $I > 2\sigma(I)$ and 0.0432 for all 1800 reflections, refining 220 parameters. Using the Hamilton significance test, (Hamilton 1965) the ratio of R -factors for the two models, using all data, is 1.16 as compared to $F_{2,1578,0.005} = 1.003$ for 1800 reflections, (dimension = 2, degrees of freedom = 1578). Therefore, the hypothesis that only two vacant sites are present can be rejected at the 0.005 level. In addition, the calculated composition using this model, refined to a formula of $\text{Fe}_{89.21}\text{S}_{96}$ or $\text{Fe}_{11.15}\text{S}_{12}$. This does not correspond to the analyzed composition of $\text{Fe}_{10.91}\text{Ni}_{0.05}\text{S}_{12}$, although it still is within the range of compositions defined by the standard deviation of the microprobe analyses.

Therefore, the structure of the 6C pyrrhotite will be reported as having four partially occupied sites in the structure instead of two. The atomic positional and anisotropic displacement parameters are given in Tables 2 and 3, with the standard errors in parentheses.

Table 4 gives the bond lengths, octahedral angular variance (OAV) and polyhedral quadratic elongation (PQE) as defined by Robinson et al. (1971), for the different octahedra surrounding the iron atoms. The latter two parameters were

TABLE 1. Crystal data and structure refinement for pyrrhotite-6C

Identification code	Pyrrhotite-6C	
Empirical formula	$\text{Fe}_{11}\text{S}_{12}$	
Formula weight	999.07	
Temperature	293(2) K	
Wavelength	0.71073 Å	
Crystal system	Monoclinic	
Space group	Fd	
Unit-cell dimensions	$a = 6.8973(15)$ Å	$\alpha = 90^\circ$
	$b = 11.954(3)$ Å	$\beta = 90.003(4)^\circ$
	$c = 34.521(7)$ Å	$\gamma = 90^\circ$
Volume	2846.2(11) Å ³	
Z	8	
Density (calculated)	4.663 Mg/m ³	
Absorption coefficient	12.585 mm ⁻¹	
F(000)	3824	
Crystal size	0.12 x 0.12 x 0.12 mm	
Theta range for data collection	3.46 to 26.36°	
Index ranges	$-8 \leq h \leq 7, -12 \leq k \leq 14, -42 \leq l \leq 20$	
Reflections collected	3186	
Independent reflections	1800 [$R_{\text{int}} = 0.0234$]	
Completeness to theta = 25.00°	98.2%	
Refinement method	Full-matrix least-squares on F^2	
Data/restraints/parameters	1800/2/222	
Goodness-of-fit on F^2	1.084	
Final R indices [$I > 2\sigma(I)$]	$R1 = 0.0288, wR2 = 0.0706$	
R indices (all data)	$R1 = 0.0371, wR2 = 0.0772$	
Absolute structure parameter	0.32(15)	
Largest diff. peak and hole	0.551 and -0.656 e-Å ⁻³	

Note: Standard errors in the tables are in parentheses and represent the last significant numbers.

TABLE 2. Atomic coordinates, occupancies, and equivalent isotropic displacement parameters for pyrrhotite-6C (space group Fd)

	x	y	z	Occ	U_{eq}
Fe1	0.1360(5)	0.1296(7)	0.0002(1)	1.000	0.028(1)
Fe2	0.1154(7)	0.1324(5)	0.0840(1)	1.000	0.023(1)
Fe3	0.1451(7)	0.1128(3)	0.1668(1)	1.000	0.019(1)
Fe4	0.1173(10)	0.1288(6)	0.2507(1)	1.000	0.029(1)
Fe5	0.1162(8)	0.1291(3)	0.3351(1)	1.000	0.018(1)
Fe6	0.1395(10)	0.1241(3)	0.4193(1)	0.898(6)	0.026(1)
Fe7	0.1196(10)	0.1223(7)	0.5034(2)	0.661(4)	0.028(2)
Fe8	0.1421(12)	0.1292(6)	0.5810(2)	0.556(5)	0.015(2)
Fe9	0.1096(8)	0.1231(3)	0.6649(1)	1.000	0.022(1)
Fe10	0.1325(10)	0.1220(5)	0.7501(1)	1.000	0.026(1)
Fe11	0.1363(8)	0.1353(4)	0.8335(1)	0.874(6)	0.018(1)
Fe12	0.1151(8)	0.1125(3)	0.9164(1)	1.000	0.020(1)
S1	0.3761(8)	0.0408(3)	-0.0422(2)	1.000	0.010(1)
S2	0.3756(9)	0.0408(3)	0.1215(1)	1.000	0.012(1)
S3	0.3781(9)	0.0419(2)	0.2926(2)	1.000	0.012(1)
S4	0.3778(8)	0.0417(3)	0.4610(2)	1.000	0.016(1)
S5	0.3762(9)	0.0415(3)	0.6257(2)	1.000	0.014(1)
S6	0.3752(9)	0.0433(2)	0.7925(2)	1.000	0.011(1)
S7	0.3750(7)	0.2075(3)	0.426(2)	1.000	0.013(1)
S8	0.3788(7)	0.2076(3)	0.2096(2)	1.000	0.014(1)
S9	0.3753(9)	0.2084(4)	0.3752(2)	1.000	0.009(1)
S10	0.3782(7)	0.2100(3)	0.5401(2)	1.000	0.013(1)
S11	0.3770(7)	0.2079(3)	0.7057(2)	1.000	0.014(1)
S12	0.3756(8)	0.2085(4)	0.8782(2)	1.000	0.011(1)

Notes: U_{eq} is defined as one third of the trace of the orthogonalized U_{ij} tensor.

¹ Deposit item AM-10-005, CIF files. Deposit items are available two ways: For a paper copy contact the Business Office of the Mineralogical Society of America (see inside front cover of recent issue) for price information. For an electronic copy visit the MSA web site at <http://www.minsocam.org>, go to the *American Mineralogist* Contents, find the table of contents for the specific volume/issue wanted, and then click on the deposit link there.

calculated by the program XtalDraw (Downs and Hall-Wallace 2003). Again, as in the case of the 5C pyrrhotite (deVilliers et al. 2009), the shortest Fe-Fe distances are along the c-axis, i.e., between face-sharing octahedra.

Part of the crystal was ground in a mortar and pestle, deposited on a low-background sample holder and examined with a PANalytical X'Pert PRO diffractometer equipped with an X'celerator detector and variable incident and diffracted beam slits. Refinement using CoK α was done using the commercial TOPAS academic software (Coelho 2007), modified by Coelho for refinement in the non-standard *Fd* space group.

The structure as described in the non-standard *Fd* setting is useful for the comparison of the different pyrrhotite structures because of the orthogonal geometry of their unit cells. However, it is not compatible with the most commonly used programs using crystallographic information, such as Rietveld refinement, electron microscopy, and materials modeling programs. The non-standard setting was therefore transformed to the conventional *Cc* setting, which also included a transformed twin relation to correspond to this setting. The *Cc* structure is related to the *Fd* structure by the transformation matrix: (1 0 0, 0 1 0, -1/2 0 1/2), with twin relation (1 0 0, 0 -1 0, -1 0 -1). Refinement of the conventional *Cc* structure gives an identical *R*-value of 0.029. The transformed unit cell and structural parameters are given in Table 5, and the atomic parameters and anisotropic displacement parameters in Tables 6 and 7.

DESCRIPTION OF THE STRUCTURE

The structure of the 6C pyrrhotite is essentially that described by Koto et al. (1975). On the examination of the superstructure reflections they proposed a structure consisting of two half-occupied iron sites together with fully occupied sites. The iron atoms are octahedrally coordinated with sulfur atoms arranged in a hexagonal close packed arrangement. They proposed an ordered arrangement where two layers containing half-occupied sites alternate with a fully occupied layer. The sequence is represented as: FDaDaFDbDbFDcDcFDdDdFDaDaF..., where Da, Db, Dc, and Dd represent defect-containing layers where the a,b,c,d sites are half-filled. This is shown in Figure 1. The outline of the structure shown in the figure is different from that used by Tokonami et al. (1972) and Koto et al. (1975) in that the origin of the structures are shifted by 1/4, 1/4, 0. This shift, first used by Wang and Salveson (2005), allows the 4C and 6C pyrrhotite

TABLE 3. Anisotropic displacement parameters ($\text{\AA}^2 \times 10^3$) for pyrrhotite-6C

	U_{11}	U_{22}	U_{33}	U_{23}	U_{13}	U_{12}
Fe1	26(2)	50(2)	9(1)	-2(1)	-1(2)	1(2)
Fe2	21(2)	32(2)	14(1)	0(1)	5(2)	7(2)
Fe3	23(2)	21(2)	14(1)	-3(1)	2(1)	3(1)
Fe4	35(3)	41(2)	10(1)	-2(1)	0(2)	-9(2)
Fe5	24(2)	17(1)	14(1)	-3(1)	2(1)	-7(2)
Fe6	36(3)	29(2)	13(2)	7(1)	1(2)	-12(3)
Fe7	29(3)	22(2)	32(3)	0(2)	-1(3)	9(3)
Fe8	15(3)	14(2)	16(3)	-6(2)	8(2)	-7(2)
Fe9	21(2)	24(2)	19(1)	7(1)	-3(2)	7(2)
Fe10	37(3)	26(2)	16(2)	-1(1)	-4(2)	7(2)
Fe11	27(3)	22(2)	6(1)	-4(1)	3(2)	-1(2)
Fe12	25(3)	24(1)	11(1)	-3(1)	-3(1)	7(2)
S1	10(2)	11(1)	8(2)	1(1)	2(2)	-1(2)
S2	15(2)	10(2)	10(2)	1(1)	4(2)	-1(2)
S3	9(2)	10(1)	16(2)	0(2)	3(2)	-3(2)
S4	9(2)	7(2)	33(2)	0(1)	6(2)	1(2)
S5	12(2)	8(2)	22(2)	-2(1)	7(2)	3(2)
S6	9(2)	11(1)	12(1)	1(2)	2(2)	-3(2)
S7	12(3)	9(2)	17(2)	-2(1)	6(2)	4(1)
S8	11(2)	10(2)	20(2)	0(1)	3(3)	1(2)
S9	10(2)	7(2)	10(2)	0(1)	2(2)	1(2)
S10	10(3)	12(2)	18(2)	1(1)	6(2)	6(1)
S11	9(2)	13(2)	18(2)	3(1)	6(2)	3(2)
S12	11(2)	7(2)	14(2)	0(1)	3(2)	0(2)

Note: The anisotropic displacement factor exponent takes the form: $-2\pi^2[h^2a^{*2}U_{11} + \dots + 2hk a^*b^*U_{12}]$.

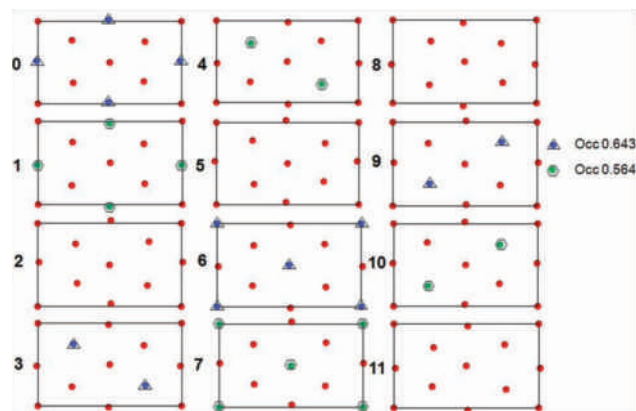


FIGURE 1. Vacancy distribution of iron in the different layers in 6C pyrrhotite as proposed by Koto et al. (1975) and refined with two partial occupancies. Two layers containing approximately half-occupied Fe sites alternate with a layer containing fully occupied sites (filled circles). The adjacent half-occupied sites always project on top of each other.

TABLE 4. Metal-sulfur bond lengths (in angstroms) of the octahedra in 5C pyrrhotite

Atom	Bond	Lengths	Atom	Bond	Lengths	Atom	Bond	Lengths
Fe1	S1	2.451(7)	Fe2	S2	2.469(7)	Fe3	S2	2.391(7)
	S3	2.520(8)		S3	2.526(6)		S4	2.399(6)
	S4	2.471(7)		S5	2.444(8)		S5	2.486(7)
	S7	2.392(7)		S7	2.460(7)		S8	2.463(7)
	S10	2.446(7)		S10	2.415(7)		S11	2.552(7)
	S11	2.478(8)		S12	2.439(7)		S12	2.522(6)
	Fe2	2.896(3)	Fe1	2.896(3)	Fe2	2.876(5)		
	Fe12	2.905(4)	Fe3	2.876(5)	Fe4	2.911(3)		
Ave. M-S		2.460			2.469			
OAV		6.118			11.678			24.762
PQE		1.0021			1.0035			1.0074
Fe4	S3	2.531(8)	Fe5	S3	2.550(8)	Fe6	S1	2.463(7)
	S4	2.458(7)		S5	2.474(7)		S4	2.398(9)
	S6	2.430(7)		S6	2.446(7)		S5	2.488(7)
	S7	2.433(7)		S7	2.445(6)		S8	2.447(6)
	S8	2.482(7)		S9	2.450(8)		S9	2.445(8)
	S11	2.462(8)		S12	2.421(7)		S12	2.519(9)
	Fe3	2.911(3)	Fe4	2.914(4)	Fe5	2.909(4)		
	Fe5	2.914(4)	Fe6	2.909(4)	Fe7	2.908(7)		
Ave. M-S		2.466			2.464			2.460
OAV		5.266			4.660			6.952
PQE		1.0017			1.0016			1.0022
Fe7	S1	2.498(9)	Fe8	S2	2.540(9)	Fe9	S1	2.459(6)
	S4	2.498(8)		S5	2.468(10)		S2	2.413(8)
	S6	2.396(8)		S6	2.456(7)		S5	2.484(8)
	S7	2.391(8)		S7	2.454(9)		S8	2.435(7)
	S8	2.534(8)		S9	2.472(8)		S9	2.441(6)
	S10	2.426(9)		S10	2.360(9)		S11	2.532(7)
	Fe6	2.908(7)	Fe7	2.864(5)	Fe8	2.909(7)		
	Fe8	2.684(5)	Fe9	2.909(7)	Fe10	2.946(3)		
Ave. M-S		2.457			2.459			2.461
OAV		6.851			12.060			11.187
PQE		1.0024			1.0038			1.0034
Fe10	S1	2.434(7)	Fe11	S2	2.481(7)	Fe12	S1	2.454(7)
	S3	2.480(8)		S3	2.531(7)		S2	2.401(6)
	S6	2.413(8)		S6	2.435(7)		S4	2.402(7)
	S8	2.464(8)		S9	2.465(7)		S9	2.464(8)
	S10	2.437(7)		S10	2.380(7)		S11	2.451(6)
	S11	2.502(8)		S12	2.423(7)		S12	2.507(7)
	Fe9	2.946(3)	Fe10	2.881(4)	Fe11	2.905(4)		
	Fe11	2.881(4)	Fe12	2.878(4)	Fe12	2.878(5)		
Ave. M-S		2.455			2.452			2.462
OAV		4.365			14.141			20.734
PQE		1.0015			1.0043			1.0062

Notes: The octahedral angular variance (OAV) is in degrees squared and the polyhedral quadratic elongation (PQE) is dimensionless. The shortest metal-metal distances are also given.

structures to be directly compared with the 5C pyrrhotite.

The above structure refines to an R -factor of 0.035 and deserves consideration despite the fact that refinement of the occupancies of four Fe sites gives a lower R -factor, which is significant at the 0.005 level, and that the composition refines to one that corresponds better with the analyzed composition. The occupancies of the two sites [Fe7 = 0.643(8) and Fe8 = 0.564(7)] refined in the structure proposed by Koto et al. (1975) are shown in Figure 1. These occupancies refine to values >0.5 and the overall composition to $\text{Fe}_{11.15}\text{S}_{12}$, which is more metal-rich than the microprobe analysis ($\text{Fe}_{10.91}\text{Ni}_{0.05}\text{S}_{12}$).

The structure where the four atomic sites are refined is shown in Figure 2. The structure is essentially the same as the one discussed above, but with two additional partially occupied sites with occupancies of 0.90 and 0.87. Apparent here is the fact that the adjacent partially occupied sites always project on top of each other. This is also the case in the 5C structure. Two

possible models were proposed by Koto et al. (1975) for this phenomenon that involved the random stacking of two layers in the structure, one containing vacancies, and one containing fully occupied sites, giving rise to the partial occupancies of 0.5. Confirmation of these models will have to wait for studies utilizing transmission electron microscopy and materials modeling techniques. These will be attempted after crystallographic studies on other pyrrhotites.

The layer occupancies of the 6C structure are also calculated and compared with the 4C and 5C layer occupancies calculated from the structures described by Tokonami et al. (1972) and de Villiers et al. (2009) respectively. This is given in Figure 3.

A comparison of the calculated powder diffraction patterns of the 5C and 6C structures is given in Figure 4. It can be seen that they are almost indistinguishable. This means that distinction and quantification of the two NC pyrrhotites is presently not likely using conventional X-ray powder diffraction methods. This was confirmed by the refinement of 6C pyrrhotite diffraction data using either the 5C or the 6C structural data. Using TOPAS, both structures gave excellent refinements using the 6C diffraction data. For the 6C structure with the 6C diffraction data, $R_{\text{wp}} = 0.017$ and $R_{\text{Bragg}} = 0.0121$, and for the 5C structure with the 6C

TABLE 5. Crystal data and structure refinement for pyrrhotite-6C (space group Cc)

Identification code	Pyrrhotite 6C-Cc	
Empirical formula	$\text{Fe}_{11.15}\text{S}_{12}$	
Formula weight	999.07	
Temperature	293(2) K	
Wavelength	0.71073 Å	
Crystal system	Monoclinic	
Space group	Cc	
Unit-cell dimensions	$a = 6.8973(15)$ Å	$\alpha = 90^\circ$
	$b = 11.954(3)$ Å	$\beta = 101.302(4)^\circ$
	$c = 17.602(4)$ Å	$\gamma = 90^\circ$
Volume	$1423.1(5)$ Å ³	
Z	4	
Density (calculated)	4.663 Mg/m ³	
Absorption coefficient	12.585 mm ⁻¹	
F(000)	1912	
Crystal size	$0.12 \times 0.12 \times 0.12$ mm ³	
Theta range for data collection	3.46 to 26.36°	
Index ranges	$-8 \leq h \leq 7, -12 \leq k \leq 14, -21 \leq l \leq 12$	
Reflections collected	3186	
Independent reflections	1800 [$R_{\text{int}} = 0.0234$]	
Completeness to $\theta = 25.00^\circ$	98.2%	
Absorption correction	Semi-empirical from equivalents	
Max. and min. transmission	0.221 and 0.210	
Refinement method	Full-matrix least-squares on F^2	
Data/restraints/parameters	1800/2/222	
Goodness-of-fit on F^2	0.971	
Final R indices [$I > 2\sigma(I)$]	$R1 = 0.0288, wR2 = 0.0726$	
R indices (all data)	$R1 = 0.0368, wR2 = 0.0801$	
Absolute structure parameter	0.516(4)	
Extinction coefficient	0	
Largest diff. peak and hole	0.514 and $-0.696 \text{ e} \cdot \text{Å}^{-3}$	

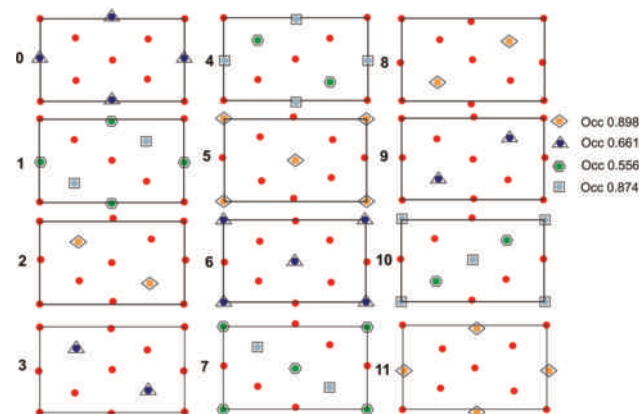


FIGURE 2. The vacancy distribution of sites in the different layers in 6C pyrrhotite. Four sites are partially occupied, with two sites that are almost fully occupied and two sites that are approximately half-filled. Layers 1, 4, 7, and 10 contain two sets of vacant sites. Fully occupied sites are shown as spheres.

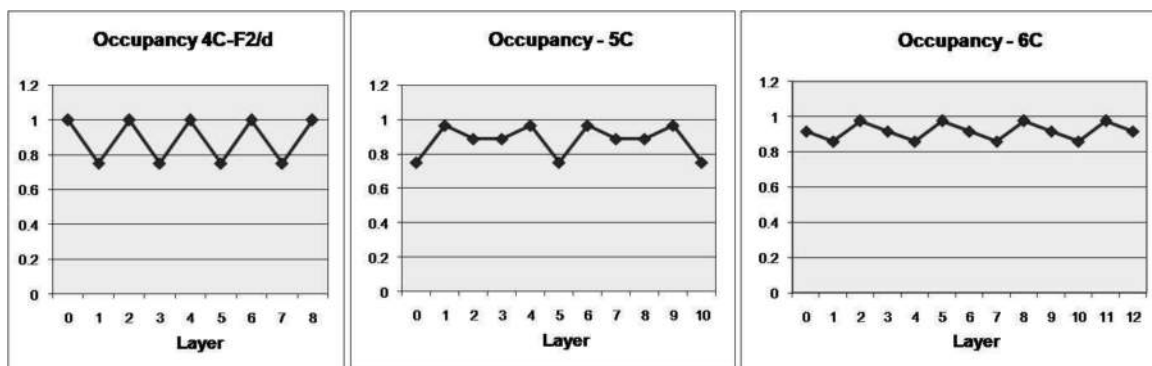


FIGURE 3. A comparison of layer occupancies in 4C, 5C, and 6C pyrrhotites. The 4C structure is the only one containing ordered vacant sites. Layers 0 and 8 in 4C, 0 and 10 in 5C, and 0 and 12 in 6C pyrrhotite are identical.

TABLE 6. Atomic coordinates ($\times 10^4$) and equivalent isotropic displacement parameters ($\text{\AA}^2 \times 10^3$) for pyrrhotite-6C (space group Cc)

	x	y	z	Occ	U_{eq}
Fe1	0.1226(5)	0.1315(6)	0.0015(2)	1.00	0.024(1)
Fe2	0.2264(7)	0.1314(5)	0.1692(2)	1.00	0.026(1)
Fe3	0.2813(6)	0.1125(3)	0.3345(2)	1.00	0.021(1)
Fe4	0.3925(8)	0.1299(5)	0.5020(2)	1.00	0.026(1)
Fe5	0.4715(10)	0.1265(3)	0.6707(2)	1.00	0.022(1)
Fe6	0.5354(9)	0.1242(3)	0.8390(2)	0.892(6)	0.024(1)
Fe7	0.6402(14)	0.1211(6)	0.0078(4)	0.667(4)	0.032(2)
Fe8	0.6983(10)	0.1293(5)	0.1632(4)	0.555(5)	0.013(1)
Fe9	0.8125(8)	0.1211(3)	0.3301(2)	1.00	0.021(1)
Fe10	0.8683(10)	0.1257(4)	0.5005(2)	1.00	0.026(1)
Fe11	0.9557(10)	0.1348(5)	0.6679(2)	0.875(6)	0.017(1)
Fe12	0.0604(8)	0.1128(3)	0.8336(2)	1.00	0.021(1)
S1	0.3409(9)	0.0416(4)	0.9240(4)	1.00	0.015(1)
S2	0.5060(9)	0.0408(4)	0.2528(3)	1.00	0.013(1)
S3	0.6723(9)	0.0436(3)	0.5866(4)	1.00	0.012(1)
S4	0.8380(9)	0.0416(4)	0.9180(4)	1.00	0.010(1)
S5	0.0040(9)	0.0409(4)	0.2449(3)	1.00	0.012(1)
S6	0.1710(9)	0.0419(3)	0.5856(4)	1.00	0.012(1)
S7	0.4180(7)	0.2089(4)	0.0824(3)	1.00	0.012(1)
S8	0.5860(8)	0.2077(4)	0.4118(3)	1.00	0.013(1)
S9	0.7580(8)	0.2086(4)	0.7571(3)	1.00	0.011(1)
S10	0.9234(8)	0.2090(4)	0.0874(3)	1.00	0.014(1)
S11	0.0899(8)	0.2089(4)	0.4209(3)	1.00	0.014(1)
S12	0.2574(7)	0.2077(4)	0.7523(3)	1.00	0.009(1)

Notes: U_{eq} is defined as one third of the trace of the orthogonalized U_{ij} tensor.

TABLE 7. Anisotropic displacement parameters ($\text{\AA}^2 \times 10^3$) for pyrrhotite-6C (space group Cc)

	U_{11}	U_{22}	U_{33}	U_{23}	U_{13}	U_{12}
Fe1	22(2)	41(2)	8(1)	-2(1)	1(2)	1(2)
Fe2	28(3)	37(2)	14(1)	1(1)	5(2)	3(2)
Fe3	19(2)	26(2)	16(2)	-5(1)	1(2)	-10(1)
Fe4	26(2)	43(2)	9(1)	1(1)	1(2)	11(2)
Fe5	29(3)	22(1)	14(2)	-3(1)	5(2)	2(2)
Fe6	28(3)	30(2)	12(2)	7(1)	0(2)	12(2)
Fe7	39(4)	28(2)	29(3)	-2(2)	6(3)	11(3)
Fe8	7(3)	11(2)	19(3)	-1(2)	1(2)	6(3)
Fe9	26(2)	19(2)	20(2)	4(1)	11(2)	-2(2)
Fe10	36(2)	24(2)	17(2)	-2(1)	1(2)	-10(2)
Fe11	26(3)	17(1)	6(1)	0(1)	-1(2)	0(2)
Fe12	32(2)	21(1)	11(1)	-5(1)	8(2)	-8(2)
S1	7(2)	7(2)	32(2)	-4(2)	5(2)	-2(2)
S2	9(2)	9(2)	22(2)	-1(2)	4(3)	-2(2)
S3	8(2)	12(1)	15(2)	-1(2)	-1(2)	6(2)
S4	11(2)	10(2)	9(2)	0(2)	0(2)	1(2)
S5	14(2)	8(2)	13(2)	-1(1)	-2(2)	4(2)
S6	9(2)	8(1)	19(2)	-3(2)	1(2)	0(2)
S7	7(2)	12(2)	13(2)	2(1)	-5(2)	-2(2)
S8	12(3)	14(2)	11(2)	3(1)	-1(2)	0(2)
S9	7(2)	10(2)	16(2)	2(2)	1(3)	-3(2)
S10	11(2)	9(2)	21(2)	0(1)	4(3)	0(2)
S11	8(2)	9(2)	24(2)	3(1)	0(3)	3(2)
S12	13(3)	7(2)	8(2)	3(1)	3(2)	-1(2)

Note: The anisotropic displacement factor exponent takes the form: $-2\pi^2[h^2a^{*2}U_{11} + \dots + 2hka^*b^*U_{12}]$.

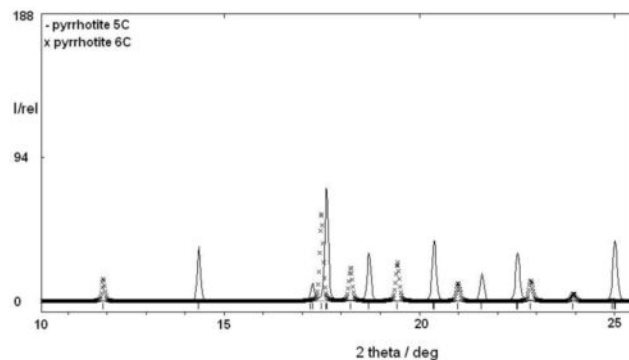
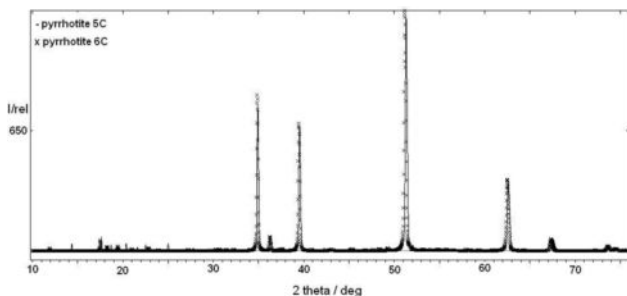


FIGURE 4. (a) Calculated powder XRD patterns of 5C (solid line) and 6C (crosses) pyrrhotite. The two patterns are almost identical except for minor peaks below $25^\circ 2\theta$. (b) Expanded XRD pattern below $25^\circ 2\theta$. The very weak unique peaks can be seen.

diffraction data $R_{\text{wp}} = 0.0188$ and $R_{\text{Bragg}} = 0.0097$.

Presently, the only reliable methods for their distinction are careful electron microprobe analysis or single-crystal X-ray methods. Rietveld methods will therefore only distinguish between 4C and 6C pyrrhotites.

ACKNOWLEDGMENTS

Donation of the single crystal by Bruce Cairncross of the University of Johannesburg is acknowledged with thanks. Because of the scarcity of good single-crystal material, this sample is especially valuable. Microprobe analysis of the sample by Peter Gräser is gratefully acknowledged. Thanks also to Alison Tuling for expert assistance with graphic challenges. Alan Coelho modified TOPAS to accommodate the non-standard space groups into the program. Thanks to him for patience and expertise.

REFERENCES CITED

- Bruker (2001) SAINT+ Version 6.45, SADABS Version 2.10. BRUKER AXS Inc., Madison, Wisconsin.
 Coelho, A. (2007) Technical Reference. TOPAS ACADEMIC, Version 4.1, July 2007.
 de Villiers, J.P.R., Liles, D.C., and Becker, M. (2009) The crystal structure of a naturally occurring 5C pyrrhotite from Sudbury, its chemistry, and vacancy distribution. *American Mineralogist*, 94, 1405–1410.
 Downs, R.T. and Hall-Wallace, M. (2003) *The American Mineralogist crystal*

- structure database. *American Mineralogist*, 88, 247–250.
 Hamilton, W.C. (1965) Significance tests on the crystallographic R factor. *Acta Crystallographica*, 18, 502–510.
 Koto, K., Morimoto, N., and Gyobu, A. (1975) The superstructure of the intermediate pyrrhotite. I. Partially disordered distribution of metal vacancy in the 6C type, $\text{Fe}_{11}\text{S}_{12}$. *Acta Crystallographica*, B31, 2759–2764.
 Morimoto, N., Gyobu, A., Mukaiyama, H., and Izawa, E. (1975) Crystallography and stability of pyrrhotites. *Economic Geology*, 70, 824–833.
 Powell, A.V., Vaquero, P., Knight, K.S., Chapon, L.C., and Sanchez, R.D. (2004) Structure and magnetism in synthetic pyrrhotite Fe_7S_8 : A powder neutron diffraction study. *Physical Review B*, 70, 014415.
 Robinson, K., Gibbs, G.V., and Ribbe, P.H. (1971) Quadratic elongation: A quantitative measure of distortion in coordination polyhedra. *Science*, 172, 567–570.
 Sheldrick, G.M. (1997) SHELX97—Programs for Crystal Structure Analysis (Release 97-2). Institut für Anorganische Chemie der Universität, Göttingen, Germany.
 Tokonami, M., Nishiguchi, K., and Morimoto, N. (1972) Crystal structure of a monoclinic pyrrhotite (Fe_7S_8). *American Mineralogist*, 57, 1066–1080.
 Wang, H. and Salveson, I. (2005) A review on the mineral chemistry of the non-stoichiometric iron sulfide, Fe_{1-x}S ($0 \leq x \leq 0.125$): polymorphs, phase relations and transitions, electronic and magnetic structures. *Phase Transitions*, 78, 547–567.

MANUSCRIPT RECEIVED MARCH 31, 2009

MANUSCRIPT ACCEPTED SEPTEMBER 10, 2009

MANUSCRIPT HANDLED BY GUOYIN SHEN